반도체디스플레이기술학회지 제19권 제3호(2020년 9월)
Journal of the Semiconductor & Display Technology, Vol. 19, No. 3. September 2020.

Understanding of RF Impedance Matching System Using VI-Probe

Ji Ha Lee[*], Hyun Keun Park[*], Jungsoo Lee[*] and Snag Jeen Hong[*†]

[*†] Department of Electronic Engineering, Myongji University, Korea

ABSTRACT

The demand for stable plasma has been on the rise because of the increased delivery power amount in the chamber for improving productivity, and fast and accurate plasma impedance matching become a crucial performance measure for radio frequency (RF) power system in semiconductor manufacturing equipment. In this paper, the overall impedance matching was understood, and voltage and current values were extracted with voltage - current (VI) probe to measure plasma impedance in real-time. Actual matching data were analyzed to derive calibration coefficient for V and I measurements to understand the characteristics of VI probe, and we demonstrated the tendency of RF impedance matching according to changes in load impedance. This preliminary empirical research can contribute to fast RF matching as well as advanced equipment control for the next level of detailed investigation on embedded system based-RF matching controller.

Key Words : RF Impedance Matching, Plasma, VI Probe, Matching Data

1. Introduction

The continuous demand for more precise control of process equipment takes place to meet the next level of circuit pattering technology; such as 3D-NAND with the emergence of additive technology [1]. Such a demands expands its scope to plasma equipment technology associated with high aspect ratio-contact (HARC) etch in 3D NAND, through silicon via (TSV), etc. Moreover, cyclic plasma process, for the instance of atomic layer etch/deposition (ALE/ALD), employs repeated plasma turn-on/off steps within a very short process step period, it requires faster and accurate plasma stability via plasma impedance matching [2-4]. Historically 13.56 MHz RF power unit and matching system is mostly preferred to generate plasma in the chamber in semiconductor manufacturing [5,6]. Process variables, such as the type of gas feed into the process chamber, gas flow rate, pressure, temperature, and RF bias, determine the plasma state, and it can be interpreted by the change of plasma impedance in terms of power delivery circuitry [7]. The modification of impedance in the plasma, consisting of resistive, capacitive, and inductive load, results in transmission power loss, signal distortion, etc. In particular, the chamber impedance changes rapidly after the plasma ignition, and RF impedance matching unit plays a crucial role to maintain 50 Ω of preset impedance between the input and output terminals. In conventional matching networks experience inevitable delays near matching points because of the innate plasma dynamics and mechanical control mechanism with variable vacuum capacitors (VVC) [8,9]. Plasma instability caused by the aforementioned delays within a short time for impedance matching affect the plasma process quality on wafer-in-process, thus it is desired to have faster and accurate RF impedance matching in plasma system by improving the performance of the RF impedance matching unit.

To alleviate the concerns of RF impedance matching, one may consider reducing latency in the mechanical control mechanism by improving the speed of VVC control in a matching network. However, fast servo loops are not practical because they can cause stability problems and

[†]E-mail: samhong@mju.ac.kr

failure to the VVC itself. It is also attempting to employ an electronic matching unit consists of capacitor arrays, but poor reliability of the capacitors in high power supply can increase the electrical signal noise depending on the operational frequencies. Therefore, the improvement of matching algorithm is the most realistic way to improve matching speed and accuracy, and the in depth understanding of RF impedance matching unit should be in the first place to prepare a forthcoming plasma process equipment in the next phase of semiconductor manufacturing technology; we may define the next phase of semiconductor manufacturing technology as Semiconductor Material, Parts, and Equipment (SMPE).

The purpose of this report is to providing entry level knowledge of RF matching units in semiconductor equipment, and some preliminary experimental procedure for impedance matching using VI-probe. Understanding of RF system begins with voltage, current, and phase information within the RF matching system, including RF power generator, RF matching unit, and load along the power transmission lines in between. We first provide some essential background theory of RF matching system with the in-situ measurement of voltage, current, and phase with VI-probe. Then, we present measured and calculated values for RF matching in the look-up tables to find the correction coefficient and how the impedance matching is performed at the load.

2. Background

When the impedance of both ends is different when connecting the input and output terminals, the maximum power cannot be delivered. According to the theory of maximum power transmission, maximum power can be delivered if the load impedance and source impedance match. The load side power consumption is W_L, the transmission side resistance is R_S, the load side net resistance is R_L, and the current flow through the circuit is i.

$$\begin{aligned} W_L &= i^2 R_L \\ &= \left(\frac{V}{R_S + R_L}\right)^2 * R_L \\ &= V^2 * \frac{R_L}{(R_S + R_L)^2} \\ &= \frac{V^2}{\left(\frac{R_{S^2}}{R_L}\right) + 2R_S + R_L} \end{aligned} \tag{1}$$

Here, set to zero for maximum differential by Z_L.

$$-\frac{R_{S^2}}{R_{L^2}} + 1 = 0 \tag{2}$$

$$R_{S^2} = R_{L^2} \tag{3}$$

Maximum power transfer is possible when R_S=R_L. The conditions for removing reflective waves from the transmitting side and transmitting them to the receiving side at maximum energy transmission efficiency are the same as the net resistance R_S on the transmitting side and the net resistance R_L on the receiving side. This is called impedance matching. The actual load or impedance of the signal source is often not a net resistance, but a reactance or capacitive load. In this case, it is necessary to match the voltage and current to absolute values and make the phases in phase [10]. The matching unit is inserted between the input and output terminals to correct the difference in impedance between the two connections, which is called impedance matching. Normally, for RF power units, the internal impedance is fixed at 50 Ω, the characteristic impedance [11]. If plasma occurs on the chamber connected to the load, the load impedance is not fixed. Changing load impedance affects the waveform of the voltage and current input, causing problems with stable plasma control. Therefore, in plasma generators it is important to use a convergence circuit to transfer maximum power without reflected power. The formulas associated with this may be organized as follows.

$$\begin{aligned} P_{ave} &= \frac{1}{2} Re[V(z) I(z)^*] \\ &= \frac{1}{2} Re\left[|V_0^+|^2 \frac{1}{Z_0}(1 - \Gamma^*(z) + \Gamma(z) \right. \\ &\qquad \left. - |\Gamma(z)|^2)\right] \\ &= \frac{1}{2}\frac{|V_0^+|^2}{Z_0} - \frac{1}{2}\frac{|V_0^+|^2}{Z_0}|\Gamma|^2 \end{aligned} \tag{4}$$

The average power applied to the load can be expressed

in terms of voltage and current as shown in (2-4). This can be expressed by two equations that show the relationship between voltage and internal impedance, and it can be expressed by the difference between the power that can appear in matched conditions and the power that has a reflection coefficient. When the load and the internal impedance satisfy the matching condition, the maximum power can be exhibited. This organized formula can be used to construct the power applied to the load by the formula of the input and the reflected power, as shown in (2-5). Here, the coefficient of reflection is defined as

$$\Gamma = (Z_L - Z_0)/(Z_L + Z_0) \tag{5}$$

$$P_0 = \frac{1}{2}\frac{|V_0^+|^2}{Z_0} \tag{6}$$

Through the formula summarized above, it is possible to formulate the change in voltage according to the change in load. As shown in Eqn. (6), the maximum power can be expressed as follows when the impedance satisfies the matching condition. The power applied to the load can be defined as follows:

$$P_L = \frac{1}{2}\frac{V_0^2}{Z_0}(1-\Gamma^2) = P_0(1-\Gamma^2) = \frac{1}{2}\frac{V_L^2}{Z_L} \tag{7}$$

P_0 represents the maximum power input, V_L represents the voltage under load, and Z_L represents the load impedance. As shown in Eqn. (7), the power applied to the load represents the difference in power reflected from the input power.

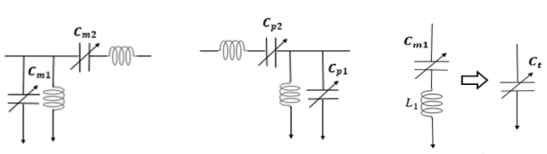

Fig. 1. Circuitry of RF matching system; (a) Most common RF matcher, (b) L-type matcher, and (c) converted parallel section.

The circuit diagram of the matcher currently in use is shown in Fig. 1. The inductor uses two fixed inductors and performs impedance matching through adjustment of the variable capacitor. Since two L-type matchers are used, the formula for calculating L-type C_1 and C_2 values is as follows C_t.

$$C_1 = \frac{1}{Z_0\omega}\sqrt{\frac{Z_0 - R}{R}}$$

$$C_2 = \frac{1}{\omega}\frac{1}{\omega L - \sqrt{R(Z_0 - R)} + X_L} \tag{8}$$

$$C_t = \frac{1}{Z_0\omega}\sqrt{\frac{Z_0 - R}{R}} \tag{9}$$

$$C_1 : \frac{1}{2\pi f(X_{L1} + X_{ct})}$$

$$C_2 : \frac{1}{\omega}\frac{1}{\omega L - \sqrt{R_L(Z_0 - R_L)} + X_L} \tag{10}$$

$$X_{C_T} = \frac{1}{2\pi f C_T} \text{ and } X_{L_1} = 2\pi f L_1 \tag{11}$$

$$X_{C_T} = X_{C_1} - X_{L_1} \text{ and } X_{C_1} = X_{C_T} + X_{L_1}\, L_1 \tag{12}$$

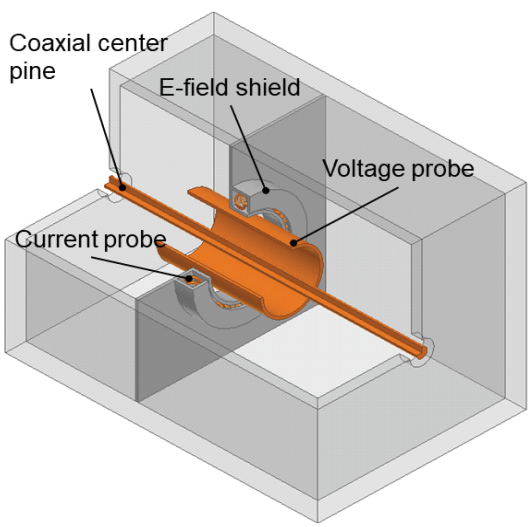

Fig. 2. An example of VI Sensor [4].

C_1 and C_2 in standard L-type are calculated as shown in Eqn. (8). Assuming the total capacitance of the parallel section is C_t, equal to Eqn. (9), $X_{Ct} = X_{C1} - X_{L1}$ as shown in Eqn. (12), expressed as $X_{C1} = X_{Ct} + X_{L1}$, and $X_{Ct} = X_{C1} - X_{L1}$ are induced by (11).

In impedance matching systems, measured voltage and current can be used to calculate impedance values [4]. When RF signal passes through coaxial cable, it is possible to get

fine signals through voltage and current detector. After converting this kind of RF analog signal to DC level, data for MCU processing can be extracted by ADC. Fig. 2 shows the inside of input sensor in 3-D to be used in the experiment. There is a conductor inside the coaxial line, and around it there is a voltage probe and a current probe. The voltage detector appears as a metal cylinder surrounding a coaxial cable with a certain radius difference. As the RF signal passes through the coaxial cable, it causes electric filed and the causing the electric field to occur, and the voltage detector to be applied electric field and an electric field is applied to the voltage detector. As a result, a voltage difference appears between the ground and the voltage sensor, and the voltage component can be detected by its measuring [2,4].

The current detector follows the basic operating principle of a toroidal coil, which is a type in which the coil is wound in the vertical direction with the magnetic flux generated around the coaxial cable. When RF signal passes through coaxial cables, magnetic field distributions occur around them according to ampere's law. The magnetic field causes AC current to flow through the coil and induces electromotive force according to Faraday's law. Current flows across both ends of the coil wound around the core, generating an EMF voltage and can obtain the current component through the EMF voltage. The E-field shield disconnects electric field couplings that can cause errors in the current detector. The measured value depends on the radius of the designed metal cylinder or the number of coils wound. Measured voltage and current signals can be predicted by calculating impedance after considering compensation variables [4].

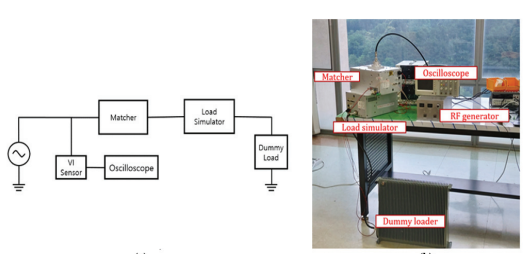

Fig. 3. Experimental apparatus: (a) A schematic diagram of hardware configuration and (b) A pictorial demonstration of the actual experimental hardware set-up.

3. Experiment method

The hardware is configured as shown in Fig. 3 (a). The RF Generator, which applies signals of 13.56 MHz, 10 to 50 W, input sensor for input voltage and current waveform measurements, two matchers, oscilloscope, and dummy load are used. One of the two matchers having a symmetrical circuit configuration is used as a matcher for impedance matching, and the other is used as a load simulator to replace the virtual plasma impedance. The load simulator and the 50 Ω dummy load are combined to form a matching target impedance. Fig. 3 (b) shows the actual equipment configuration.

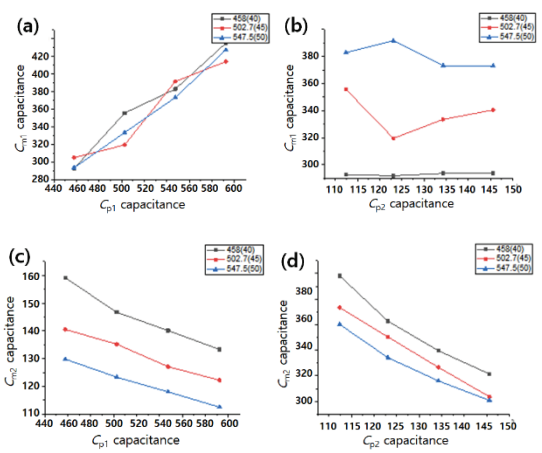

Fig. 4. Graph of capacitance change; (a) Fixed load C_{p2}, change matcher C_{m1}, (b) Fixed load C_{p1}, change matcher C_{m1}, (c) Fixed load C_{p2}, change matcher C_{m2}, and (d) Fixed load C_{p1}, change matcher C_{m2}.

Table 1. Look Up Table at 10W

Load Simulator		OSC			Matching data	
C1 (pF)	C2 (pF)	V (mV)	EMF (mV)	Phase	C1 (pF)	C2 (pF)
367.8 (30)	180 (70)	Out of range (rp:0.3)				
458 (40)	156.9 (60)	68.0	37.0	0~6	303.2 (23)	120.2 (44)
547.5 (50)	134.3 (50)	70.1	37.9	05~12	391.6 (33)	122.2 (45)
637.1 (60)	112.4 (40)	70.7	40.3	4.7~7.2	490 (44)	133.3 (50)
683.3 (65)	101.1 (35)	70.2	38.7	6.9~9.9	537.2 (49.3)	146.5 (55.7)
728.5 (70)	90 (30)	67.8	37.3	4.8~7.2	588.0 (55)	167.8 (65)
819 (80)	67.2 (20)	Out of range (10)				

Table 2. Look Up Table at 20W

Load Simulator		OSC			Matching data	
C1 (pF)	C2 (pF)	V (mV)	EMF (mV)	Phase	C1 (pF)	C2 (pF)
367.8 (30)	180 (70)	Out of range(rp:0.4)				
458 (40)	156.9 (60)	100.1	55.3	4.3~8.1	239.6 (22)	117.8 (43)
547.5 (50)	134.3 (50)	102.0	55.1	06~26	391.6 (33)	121.6 (44.7)
637.1 (60)	112.4 (40)	99.8	55.7	10.5~17.7	490 (44)	133.3 (50)
683.3 (65)	101.1 (35)	100	54.6	03 ~12	537.2 (49.3)	146.5 (55.7)
728.5 (70)	90 (30)	99.6	56.0	12 ~14.5	588.0 (55)	167.8 (65)
819 (80)	67.2 (20)	out of range (19.9)				

Table 3. Look Up Table at 30W

Load Simulator		OSC			Matching data	
C1 (pF)	C2 (pF)	V (mV)	EMF (mV)	Phase	C1 (pF)	C2 (pF)
367.8 (30)	180 (70)	Out of range(rp:0.5)				
458 (40)	156.9 (60)	123.0	68.3	10~15	293.6 (22)	120.1 (44)
547.5 (50)	134.3 (50)	126	66.8	5.4~11.2	391.6 (33)	122.2 (45)
637.1 (60)	112.4 (40)	125.3	69.4	10~18.1	490 (44)	133.3 (50)
683.3 (65)	101.1 (35)	121.3	66.6	10.5~14.3	537.2 (49.3)	146.5 (55.7)
728.5 (70)	90 (30)	125.6	68.8	9.1~12.9	588.0 (55)	167.8 (65)
819 (80)	67.2 (20)	Out of range (30)				

Table 4. Look Up Table at 40W

Load Simulator		OSC			Matching data	
C1 (pF)	C2 (pF)	V (mV)	EMF (mV)	Phase	C1 (pF)	C2 (pF)
367.8 (30)	180 (70)	Out of range (rp:0.7)				
458 (40)	156.9 (60)	161.3	87.3	9~13	293.6 (22)	120.1 (44)
547.5 (50)	134.3 (50)	161.5	88.6	13~22	391.6 (33)	122.2 (45)
637.1 (60)	112.4 (40)	157	87.4	18.1~20 .7	490 (44)	133.3 (50)
683.3 (65)	101.1 (35)	159	87.1	9.7~11. 1	537.2 (49.3)	146.5 (55.7)
728.5 (70)	90 (30)	159.3	88.2	16.5 ~17.9	579.3 (54)	167.8 (65)
819 (80)	67.2 (20)	Out of range (10)				

To proceed with the matching of various load impedance, convert the value of the load impedance using the step motor connected to the VVC of the load simulator. In this experiment, the power source of 10, 20, 30, and 50 W is matched based on the reflection power of zero. The following table shows the RMS voltage and current, phase, and matcher VVC values measured by oscilloscope. At this time, the theoretical voltage and current ratio should appear to be 50, but the actual RMS measurement ratio will not be 50. Therefore, the measured data analysis draws compensation values that adjust the voltage current ratio to 50 and progresses the trend analysis.

The experiment found the measured V and I values at each matching point as load impedance changed at 10 W, 20 W, 30 W, and 50 W. However, the experiment found a matching point with the reflect power displayed on the generator but determined that the phase was not valid due to the oscilloscope's performance problems. At this time, the difference between the theoretical V and I values existed, so when the characteristics of the VI sensors in use were found out the difference, the weight of V averaged 0.326 and the weight of I was averaged 0.011. If the capacitors of the load (C_{p1}, C_{p2}) were fixed to reduce the variables and determine the significance of the experiment, tabulation of the values of capacitors (C_{m1}, C_{m2}) at each location was the same as Figs. 4 (a)-(d). and all three experiments had similar results, so the significance of the experiment could be determined.

In addition, the following table was redrawn to reduce the variables and identify their correlation. As a result, it was determined that C_{m1} was unchanged due to changes in C_{p2} (change in load impedance) when C_{p1} was fixed, and that only C_{m2} had an effect on matching. However, when C_{p2} was fixed, it was found that the relationship between C_{m1} and C_{m2} existed due to changes in C_{p1} (the change in impedance of the load).

3. Conclusion

In this report, we present fundamental understand of RF impedance matching in conventional semiconductor equipment to encourage the novice to RF engineering in SMPE. Under the university educational research environment, we have set-up an experimental apparatus for RF network with resistive dummy load, and we have measured impedance change according to the position of

VVC inside the matching unit. The summarized theory maybe a redundancy of the well-known textbook, but it is worthwhile to provide in this report for the convenient review on the relative theory for the novice to RF impedance units. The provided experimental apparatus is useful to undergraduate level of electrical engineers to learn RF matching unit of semiconductor equipment, and the suggested method for the practice of impedance matching is also valuable to provide fundamental understanding of impedance matching unit by the control of VVC.

Acknowledgement

This work was supported by LINC+ Semiconductor Equipment Engineering program in Myongji University granted funded by Ministry of Education and Korea Institute of Advanced Technology (KIAT) grant funded by Korea Government (MOTIE). (P0008458, The Competency Development Program for Specialist.) Authors are grateful to Mr. Hong at COMET Technologies Korea for the endeavored student mentoring as well as the RF components support.

Reference

1. H. Sugai and K. Nakamura, “Recent Innovations in Microwave Probes for Reactive Plasma Diagnostics,” *Jpn. J. Appl. Phys*., Vol. 58, No. 6, pp. 060101:1-19, 2019.
2. J. Kim and S. W. Lee, “Impedance Matching Method and Impedance Matching System,” *Kor. Patent* 10-1544975, Aug.,10, 2015.
3. Y. Lee, W. Song and S. J. Hong, “In situ monitoring of plasma ignition step in capacitively coupled plasma systems,” *Jpn. J. Appl. Phys*., Vol. 59, No. JS, pp. SJJD02:1-6, 2020.
4. Y. C. Jang, S. H. Park, S. M. Jeong, S. W. Ryu, G. H. Kim, “Role of Features in Plasma Information Based Virtual Metrology (PI-VM) for SiO2 Etching Depth,” *J. Semi. Disp. Technol.*, Vol. 18, No. 4, pp. 30-34, 2019.
5. K. H. Jang, S.-Y. Park, J.-J. Cho, and D.-H. Lee “Error Rate Enhancement Algorithm for 13.56 MHz Impedance Automatic Matching System,” *J. Kor. Inst. Electromagnetic Eng. Sci.*, Vol. 29, No. 7, pp. 55-60, 2020.
6. H.C. Wang and H.I. Seo, “RF Loss Miniaturization Method Using High Impedance Filter for Research,” *J. Semi. Disp. Technol.*, Vol. 19, No. 1, pp. 30-34, 2019.
7. J. H. Kim, S.W. Lee, and Y. K. Lee, “Impedance Matching Method and Electrical Equipment for this Method,” *Kor. Patent* 10-0895689, April, 23, 2009
8. N. Manabu and H. Naoya “Matcher and matching method,” *Kor. Patent* 10-1829563, Feb, 24, 2015
9. S. M. Rossnagel, “Sputter Deposition for Semiconductor Manufacturing,” *IBM J. Research and Development*, Vol. 43, No. 1.2, pp. 163-179, 1999.
10. D. K. Choi, C. Y. Won, “High Frequency Power Unit and Impedance Matching,” *The Korean Institute of Illuminating and Electrical Installation Engineers*, pp.23-28, 2002
11. H. C. Wang and H. I. Seo, “RF Loss Minimization Method Using High Impedance Filter for Research,” *J. Semiconductor & Display Technology*, Vol. 19, No. 1, pp. 56-60, 2020.

접수일: 2020년 8월 26일, 심사일: 2020년 9월 7일,
게재확정일: 2020년 9월 11일